

Geometric Correction for Projected Image on Patterned Screen

[Rintaro Imai Tsukasa Kato Ryo Taguchi Masahiro Hoguro Taizo Umezaki]

Abstract— In recent years, projection device which has advanced its miniaturization and price reduction are attracted as display device against a backdrop of high needs for wide and high-definition screen. However, the expression of projector on non-special screen causes geometric problems of distorted expression caused by a surface shape of the screen and a positional relation among devices. To solve these problems, a lot of methods have been our proposing by regarding a camera device as a viewer, transforming input projector images based on acquired images by a camera device. In this paper, we propose fast geometric correction method with easy calculation by using only Gray code pattern, and show that new method is robust for design patterns of screen by evaluation experiment.

Keywords—geometric correction, color correction, projector-camera system, calibration

I. Introduction

In recent years, the projecting technique on curtains and walls in offices and living rooms has been drawing attention by using projection devices which have advanced their miniaturization and price reduction against a backdrop of high needs for wide and high-definition screens. However, the display of a projector on general purpose screen causes the following two problems: The first is a geometric problem of distorted expression caused by the surface shape of the screen and a positional relation among the screen, the projector, and the viewer. The second is photometric problem, that is, brightness and tint of the expression look different because of non-homogeneous reflectance characteristic of the screen. To solve these problems, a lot of methods have been our proposing by using a projector-camera system. The projector-camera system brings geometric correction and photometric compensation, by regarding a camera device as a viewer, and transforms input projector images based on acquired images by a camera device. For example, the geometric correction methods our proposing in [1][2] use projecting slit patterns and capturing by a camera device. Geometric correction process is very important to retain the accuracy of photometric compensation, because the correction precedes the compensation. However, the research of the influence for correction on the non-homogeneous reflectance screens has never taken notice of. In this paper, we propose the geometric correction using Gray code patterns and verify that the method decreases correction errors compared with the conventional method using slit patterns.

Rintaro Imai, Tsukasa Kato, Ryo Taguchi, Taizo Umezaki
Nagoya Institute of Technology
Japan
imai@ume.mta.nitech.ac.jp

Masahiro Hoguro
Chubu University

II. Experimental Equipment

The projector-camera system on this research consists of a projecting device, a camera, a computer for image processing, and a projection screen. Appearance of this equipment is shown in Fig. 1. This system requires that the equipment should be located indoors, all the components of system should be kept stationary, and the surface shape of the screen is assumed to be smoothly curved. The camera device we have used is IMAGING SOURCE DFK61BUC02 with a resolution of 2560x1536pixel. The projector we have used is EPSON EB-1770W with resolution of 640x384pixel.

III. Geometric Correction Method

A. Gray Code Pattern and Centroid

To obtain non-distorted images by considering the camera as a viewer, it is necessary to determine 2D mapping between displayed and acquired images. In our proposing method, we use complementary Gray code patterns expected efficiency and the reduction of coding errors [5]. Examples of Gray code patterns are shown in Fig. 2. The projector displays patterns, one at a time, and the camera device captures the displayed pattern images. Two-dimensional space codes are assigned to input and acquired images by decoding captured patterns. Note that bit depth and pixel-width of each code are variable depending on the system configuration. From Eq. (1) and (2), let $G_{i,j}$ and $S_{i,j}$ be the centroids of the area assigned for two-dimensional code (i, j) on input and acquired images respectively. Here, $A(i, j)$ is the area assigned code (i, j) on acquired image, and $B(i, j)$ is the one on input image.

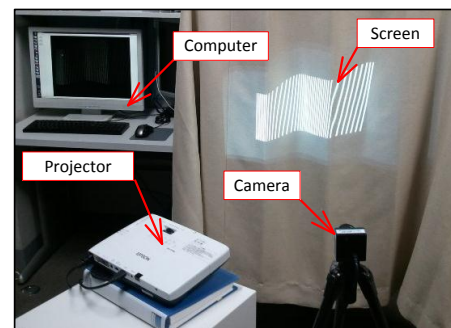


Figure 1. Appearance of experiment equipment.



Figure 2. Complementary Gray code patterns for horizontal and vertical direction.

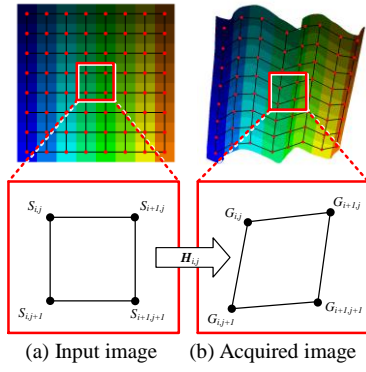


Figure 3. Mesh corresponding.

Finally, we obtain corresponding points coordinated between two images by identifying $G_{i,j}$ with $S_{i,j}$.

$$G_{i,j} = \frac{1}{|A(i,j)|} \sum_{(x,y) \in A(i,j)} (x,y), \quad (1)$$

$$S_{i,j} = \frac{1}{|B(i,j)|} \sum_{(x,y) \in B(i,j)} (x,y). \quad (2)$$

B. Mesh and Correction Table

The shape of the screen is approximated as mesh generated of 4 adjacent corresponded points in the preceding paragraph. Meshes in input and acquired image are corresponded by perspective transform. Let $G=(x, y)$ be a point on the acquired images and $S=(X, Y)$ be a point on the input image. A perspective transform which maps G to S are expressed as Eq. (3) and (4).

$$X = \frac{h_1 x + h_2 y + h_3}{h_7 x + h_8 y + 1}, \quad (3)$$

$$Y = \frac{h_4 x + h_5 y + h_6}{h_7 x + h_8 y + 1}, \quad (4)$$

$$\begin{pmatrix} X \\ Y \end{pmatrix} = \begin{pmatrix} x & y & 1 & 0 & 0 & 0 & -xX & -yX \\ 0 & 0 & 0 & X & Y & 1 & -xY & -yY \end{pmatrix} \cdot \begin{pmatrix} h_1 \\ \vdots \\ h_8 \end{pmatrix}. \quad (5)$$

Here h_1, \dots, h_8 are the elements of the perspective transformation matrix. From the correspondence between points G and S , we obtain restriction in Eq. (5). Due to the degree of freedom of the equation is 6, we can determine the transformation matrix by at least 4 correspondences between 2-points. Hence, perspective transformation $H_{i,j}=(h_1, \dots, h_8)$ that maps quadrilateral $G_{i,j} G_{i,j+1} G_{i+1,j+1} G_{i+1,j}$ to quadrilateral $S_{i,j} S_{i,j+1} S_{i+1,j+1} S_{i+1,j}$ can be estimated such as shown in Fig. 3. Then, by composing local transformation defined on each mesh, we can construct the correction table from input images to acquired images. Thus, we can observe non-distorted images by transforming the original image geometrically based on the table.

C. Slit Pattern Method

We describe the conventional method, i.e., slit pattern method. Slit pattern consists of horizontal and vertical white lines queued at uniform interval. The projector displays

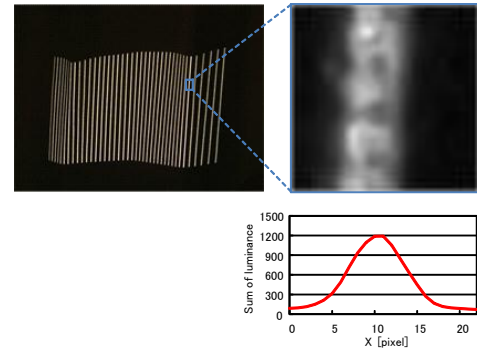


Figure 4. Slit and luminance projection for vertical direction.

pattern images shifted by 1 pixel. Each point on input and acquired images are corresponded by calculating cross point of slits. The, we obtain geometric correction table. Cross points of slits in acquired image are calculated as the following way. First, to get rough location of slits, two-dimensional codes are assigned by projecting-capturing Gray code patterns whose pixel-width is equal to the slit interval. Luminance projection area is determined by the centroids of adjacent codes. In the case of vertical slit, luminance projection goes along Y -direction. Fig. 4 shows local image for projection luminance and result of projected distribution. The maximum point of projected distribution is X -component of cross point of slits. Note that this maximum point is sub-pixel peak of approximated quadratic polynomial from the projection distribution.

IV. Experiment of Geometric Correction

We have experimented out proposing method and the conventional method. In this experiment, we use unpatterned curtain as shown in Fig. 5. In our proposing method, pixel-width of each code for Gray code pattern is 4pixel, and all patterns besides complementary pattern total 36. In conventional method, white lines of 3pixel wide queue at 16pixel intervals in slit pattern. Moreover, pixel-width of each code for Gray code pattern to detect cross points stably is 16pixel. Thus, all patterns in conventional method total 60. The results of this experiment are shown in Fig. 6. The uncorrected results (b) have distortion caused by the bend of curtains and positional relation among devices. On the other hand, corrected results (c) and (d) by both methods look very similar to the original image (a). And apparent difference can't be observed between the two methods. Therefore both methods seem to have same ability of correction.

Next, we discuss the processing time for correcting. In this experiment, wait time from displaying a pattern until capturing is 350msec. CPU of computer for calculation is Core i7 3.40GHz. In conventional method, it takes 21.2sec for displaying and capturing 60 patterns, and 35.1sec for calculating cross point and constructing correction table, thus total processing time is 56.3sec. In our proposing method, it takes 12.5sec for displaying and capturing 36 patterns, and 520msec for generating mesh and constructing correction table. Therefore total time is 13.1sec. Time is significantly reduced in comparison with the conventional method.

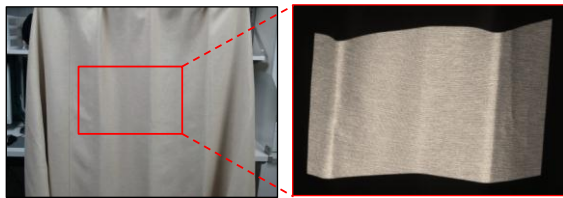
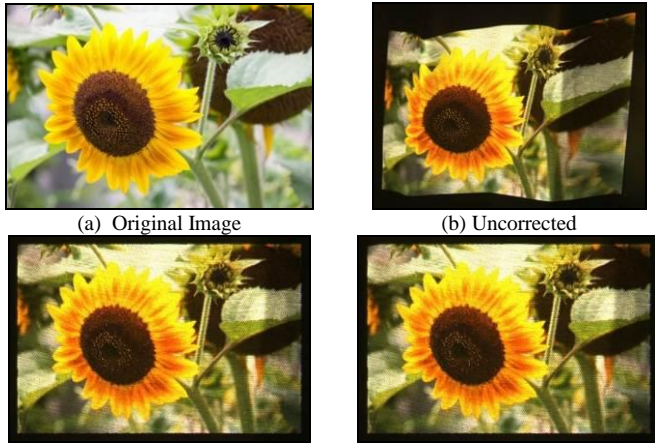


Figure 5. Unpatterned curtain and its acquired image.



(a) Original Image

(b) Uncorrected

(c) Corrected in the our proposing method

(d) Corrected in the conventional method

Figure 6. Results of geometric correction.

Note that decoding process for Gray code is executed in the background while displaying and capturing.

The reason why processing time is shortened in our proposing method is fewer patterns are used. In addition, computational complexity and number of image accessing increase compared to our proposing method, because it is necessary for conventional method to execute luminance projection as shown in Fig. 4 and polynomial fitting on each point. To shorten processing time for correction, it is effective to parallelize process on GPU, to use high speed camera, and to synchronize camera and projector devices. We will think about shortening time in future work.

v. Evaluation Results

A. Correction Accuracy on Unpatterned Screen

We evaluated difference between our proposing and conventional method on unpatterned screen, and prove that both methods have same accuracy of geometric correction. In this experience, we used the same curtain as the previous experiment (Fig. 5). True value of the evaluation is the correction table in the conventional method. We evaluate the error of correction table in our proposing method. This error is calculated by Euclidian distance. Hence, we evaluate on input image coordinate, not on acquired image coordinate. For example, Fig.7 shows transformed acquired image of the curtain on input image coordinate. Pixel-widths of each code for Gray code pattern are 32, 16, 8, and 4pixel, and we evaluate them respectively. The 2D error distributions expressed by monotone are shown in Fig. 8.



Figure 7. Transformed acquired image of unpatterned curtain on input image coordinate.

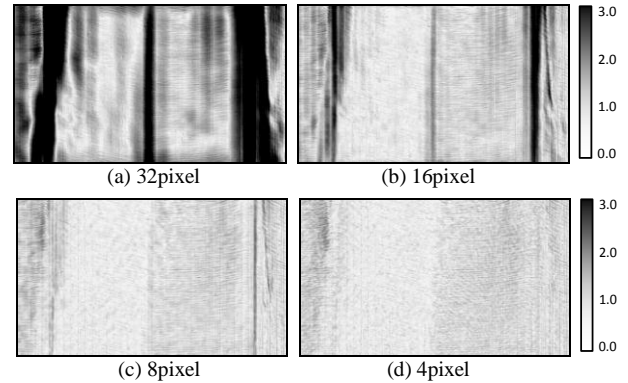


Figure 8. Errors distribution with each pixel-width.

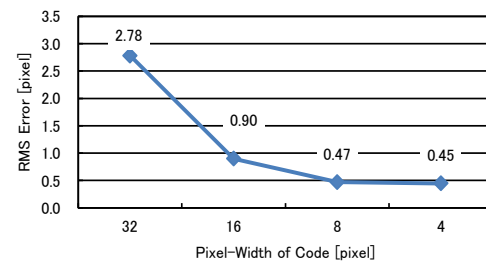


Figure 9. RMS errors with each pixel-width.

The change of RMS errors is shown in Fig. 9. In Fig. 8 (a), large error appeared around the bend of curtain in the case of 32pixel-width is going to shrink as pixel-width is getting smaller. This cause is considered that rough mesh with large pixel-width does not reflect abrupt shape change of screen. As shown Fig. 9, RMS error decreases rapidly for 16pixel-width. The lowest error is 0.45pixel in the case of 4pixel-width. Therefore, the two methods have the same accuracy of correction on unpatterned screen.

B. Influence for Correction Accuracy on Patterned Screen

We evaluate the influence of patterns of screen for accuracy of correction. In this experiment, we used the flat place with drawings of some color squares shown in Fig. 10. Each square is colored respectively with red, blue, yellow and green from upper-left, fine gray, purple, pink and dark gray from lower-left. True value of evaluation is the correction table which is calculated from perspective transformation consists of 4points shown in Fig. 10. This table is independent of design of plate. Fig. 11 shows transformed acquired images based on this correction table. We evaluate the error of correction table in our proposing and the conventional method. This error is calculated by Euclidian distance. The patterns

used in this experiment are the same in chapter 4. Fig. 12 shows the error distributions expressed by monotone and distribution on $X=360, 520$. On $X=520$, maximum error is 3.48pixel in the conventional method, while it is 1.45pixel in our proposing method. The error reduced to 42%. Therefore, our proposing method is robust for change of design of screen in comparison to the conventional method. However, as seen from 2D error distribution for our proposing method, moire-like periodic error occurred. Errors in the conventional method in Fig. 12 (a) change smoothly. On the other hand, errors of our proposing method in (b) change with amplitude of high-frequency. Error distribution contains beats caused by the difference between spatial frequency of resolution of camera and projector. Mesh-approximate seems to emphasize the beat. TABLE I shows RMS errors of 2 methods respectively. RMS error reduced in our proposing method, so that, it seems that the influence of beat on the whole accuracy of correction is small. We will think about analyzing and improving the influence of this phenomenon in future work.

The reason why such large error occurs in the conventional method is projection distribution distorts when a slit crosses border of design patterns. Fig. 13 shows the example of projection distribution around border and interior of design patterns.



Figure 10. Colored plate.

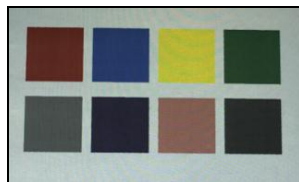
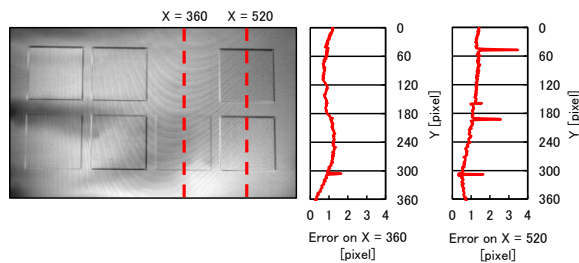
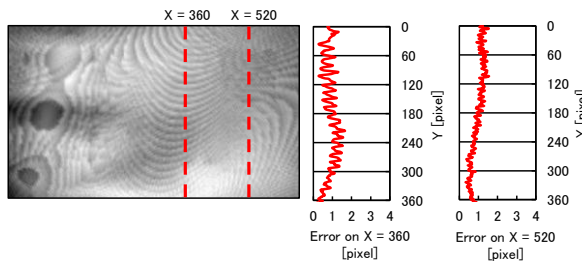


Figure 11. Transformed acquired image of colored plate on input image coordinate.



(a) Conventional method



(b) Our proposing method

Figure 12. Error distributions of geometric correction on plate.

TABLE I. RMS ERRORS OF GEOMETRIC CORRECTION ON PLATE

	Conventional Method	Our Proposing Method
RMS Error [pixel]	1.10	1.06

While the distribution in Fig. 13 (b) seems symmetric, the distribution in (a) seems asymmetric and draws to side of white area. After all, the maximum peak of distribution shifts to positive direction along X-direction. On the other hand, the reason why large error does not appear on the border is influence for the change of design patterns reduces by using complementary Gray code patterns.

Next, we evaluate differences between the conventional and our proposing method on patterned curtain shown in Fig. 14. In this experiment, true value is correction table in conventional method. We evaluate the error of correction table in our proposing method. This error is calculated by Euclidian distance. The patterns used in this experiment are the same in chapter 4. Fig. 16 shows error distribution expressed by monotone and error on $Y=192$. From error distribution in Fig. 16, large error occurs on the border of design patterns. The maximum error is 1.30pixel on $Y=192$. Then, to judge which method is more affected by design patterns, we verify the gradient of each correction table. Because the curtain we have used seems to be smoothly curved, the gradient must distribute smoothly on the border of design if it is not affected by design patterns. Let $k = (s+t)/2$ be a scalar gradient on point (x, y) on the correction table. Here, s and t are the length of gradient vector for X and Y direction respectively as the following:

$$s(x, y) = \|R(x+1, y) - R(x, y)\|, \quad (6)$$

$$t(x, y) = \|R(x, y+1) - R(x, y)\| \quad (7)$$

$R(x, y)$ is the point on acquired image corresponding to a point (x, y) on correction table, and $\| \cdot \|$ is norm function lead by Euclidian distance on linear real plane. Fig. 17 shows the gradient distribution expressed by monotone in the conventional and our proposing method and their enlarged images. In the conventional method, the gradient of correction table changes on the border of design patterns. On the other hand, such change of gradient can't be appeared in our proposing method and it distributes smooth. Therefore, likewise the result of experiment on colored plate, our method is more robust for the change of design than the conventional method on screen with smooth curve such as a curtain.

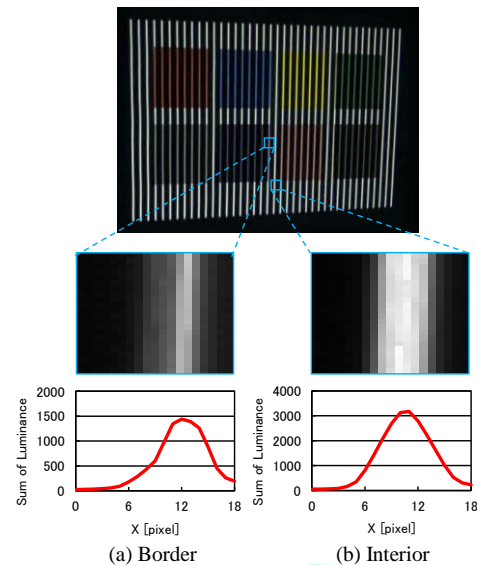


Figure 13. Projection distributions around design pattern.





Figure 14. Patterned curtain and its acquired image.



Figure 15. Transformed acquired image on input image coordinate of patterned curtain.

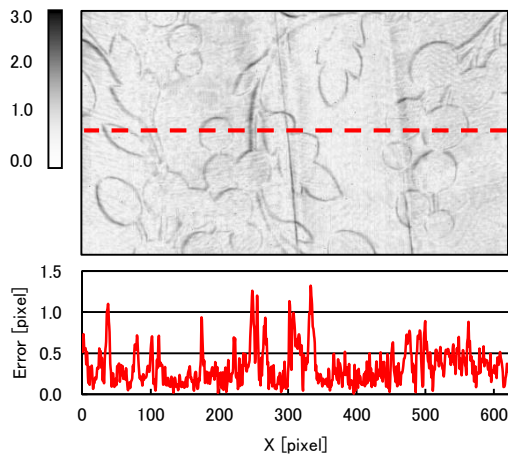
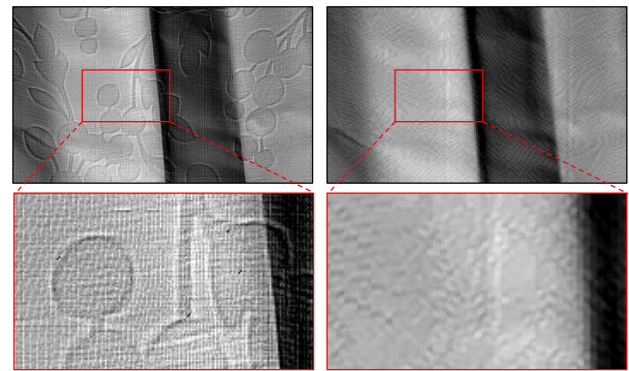


Figure 16. Error distribution of geometric correction on patterned curtain.

VI. Luminance Compensation

Finally, we experiment on simplified grayscale luminance compensation by using geometric correction, and show that accuracy of compensation rises in the case of our proposing method. Process of luminance correction is the following. First, projecting and capturing uniform images whose luminance is from 0 to 255, and transforming them to input image coordinate. Then, we plot luminance for 256 images on each point, and smooth this table with the moving average and monotonize. Therefore, to compensate luminance, that is, to make input image to obtain desired acquired image, we can refer this table in reverse on each point. We evaluate the accuracy of compensation by calculating PSNR (Peak signal-to-noise ratio) between shading compensated images and uniform images. In the evaluation experiment, screen is the colored plate used in chapter 5. Fig. 18 shows results of luminance compensation based on geometrical correction table in the conventional and our proposing methods. Fig. 19 and TABLE II show PSNR in the whole screen of each shading

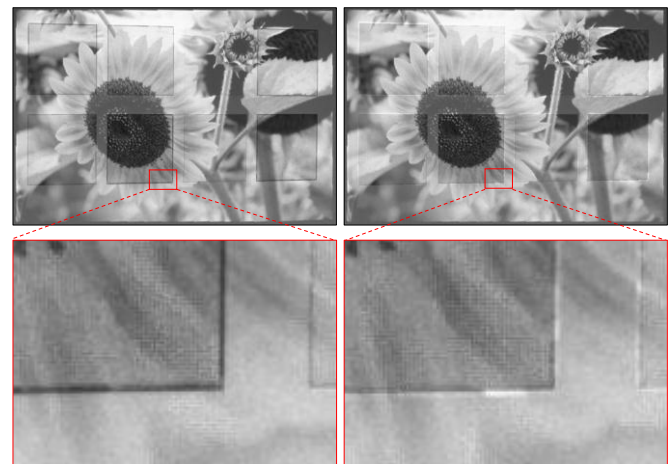


(a) Conventional method (b) Our proposing method

Figure 17. Gradient of geometric correction table.



(a) Uncompensated (b) Compensated input image



(c) Compensated in the conventional method (d) Compensated in our proposing method

Figure 18. Results of luminance compensation.

luminance. In Fig. 18 (c), luminance around the border of square decreased. This cause is that projection distribution draws to the bright area as explained in paragraph 5.2, so that the square looks small the in projected image. On the other hand, in (d) our proposing method, luminance gap around the border is alleviated because our proposing method has more high-accuracy of geometric correction. As shown in Fig. 19, the relation between compensated luminance and PSNR is the greatest when compensation luminance is equal to environmental light, and falls after that, that is, the accuracy of compensation gets worse. On the range from 25 to 100, the accuracy in our proposing method gains an advance. Note that squares with dark colors are not compensated well because of the secondary reflection on screen. We have same experiment on the patterned curtain, and confirmed that PSNR rises barely in our proposing method

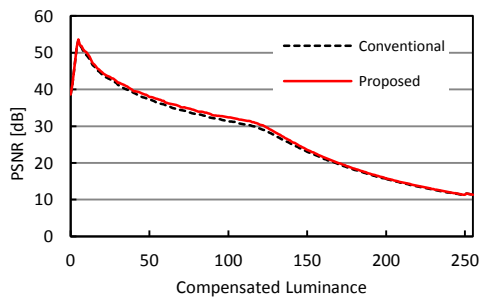


Figure 19. Shading luminance compensation and PSNR.

TABLE II. SHADING LUMINANCE COMPENSATION AND PSNR [dB]

Compensated Luminance	Conventional Method	Our proposing Method
50	37.3	37.9
100	31.3	32.4
150	23.2	23.5

VII. Conclusion

In this paper, we our proposing fast geometric correction method with easy calculation, and showed that new method is robust for the change of design patterns of screen by evaluation experiment. It seems possible to improve accuracy of photometric correction after geometric correction. We will consider reducing method for correction error with periodicity and more hi-accuracy photometric correction by analyzing influence of design patterns for geometric correction.

References

- [1] Oliver Bimber, Andreas Emmerling, Thomas Klemmer, "Embedded Entertainment with Start Projectors", IEEE Computer, vol.38, no.1: pp.48-55, 2005.
- [2] Toru Takahashi, Mamoru Miura, Koichi Ito, Takafumi Aoki, "Geometric Correction for Projected Images Using High-Accuracy Stereo Vision Based on Phase-Only Correlation", IEICE TRANSACTIONS on Information and Systems, vol.J94-D, no.8: pp.1387-1397, 2011.
- [3] Michael D. Grossberg, Harish Peri, Shree K. Nayar, Peter N. Belhumeur, "Making one object look like another: controlling appearance using a projector-camera system", In Proceedings of CVPR 2004: pp.452-459, 2004.
- [4] Mark Ashdown, Imari Sato, Takahiro Okabe, Yoichi Sato, "Perceptual Photometric Compensation for Projected Images", IEICE TRANSACTIONS on Information and Systems, vol.J90-D, no.8: pp.2115-2125, 2007.
- [5] S. Inokuchi, K. Sato, F. Matsuda, "Range imaging system for 3-D object recognition", In Proceedings of the International Conference on Pattern Recognition, pp.806-808, 1984.

About Authors:



Rintaro Imai received the B.E. and M.E. degrees in mathematics from Saitama University, Japan, in 2009 and 2012. Currently, he is a Ph.D. candidate in computer science and engineering at Nagoya Institute of Technology, Japan. His research interests are projecting technology and three dimension measurement. He is a student member of IEICE.



Tsukasa Kato received the B.E. degree in electrical engineering and computer science, and the M.E. degree in techno-business administration from Nagoya Institute of Technology, Japan, in 2010 and 2011. Currently, he is a Ph.D. candidate in computer science and engineering at Nagoya Institute of Technology. His research interests are image processing and three dimension measurement. He is a student member of IEICE.



Ryo Taguchi received the B.E., M.E. and Ph.D. degrees in computer science and engineering from Toyohashi University of Technology, Japan, in 2002, 2004 and 2008. He has been an Assistant Professor at Nagoya Institute of Technology since 2008. His research interests are conversation with robot and language acquisition. He is a member of JSAI, IPSJ, RSJ and ASJ.



Masahiro Hoguro received the B.E. and M.E. degrees in electrical engineering from Chubu University, Japan, in 1993 and 1995. In 2009, he received the Ph.D. in computer science and engineering at Nagoya Institute of Technology. He has been an Associate Professor at Chubu University since 2010. His research interests are speech and image processing. He is a member of IEICE and JSWE.



Taizo Umezaki received the B.E. degree in computer science from Toyohashi University of Technology, Japan, in 1982. He received the Ph.D. degrees in computer science from Nagoya University, Japan, in 1987. In 1990 he was a lecture and in 1992 an assistant professor. During 1993-1987 he was Visiting Scholar at Carnegie Mellon University. He was a Professor at Chubu University in 1999. Since 2003 he has been a Professor at Nagoya Institute of Technology. His research interests are speech and image processing, education for deaf children, and welfare robot. Dr. Taizo Umezaki received the best paper award from JSWE in 2003, and won the Good Design Award 2006. He is a member of IPSJ, ASJ, IEICE, JSWE, HIS of Japan, JSMBE, RSJ and JSPE.